

Phylogenetic Relationships among Agamid Lizards of the *Laudakia caucasia* Species Group: Testing Hypotheses of Biogeographic Fragmentation and an Area Cladogram for the Iranian Plateau

J. Robert Macey,* James A. Schulte II,* Natalia B. Ananjeva,† Allan Larson,*¹
Nasrullah Rastegar-Pouyani,‡ Sakhat M. Shammakov,§ and Theodore J. Papenfuss¶

*Department of Biology, Campus Box 1137, Washington University, St. Louis, Missouri 63130-4899; †Zoological Institute, Russian Academy of Sciences, 1 Universitetskaya nab., St. Petersburg 199034, Russia; ‡Department of Zoology, Göteborg University, Medicinaregatan 18, S-413 90, Göteborg, Sweden; §Institute of Zoology, Turkmenistan Academy of Sciences, Azadi Street 6, 744000 Ashgabat, Turkmenistan; and ¶Museum of Vertebrate Zoology, University of California, Berkeley, California 94720

Received July 29, 1997; revised October 16, 1997

Phylogenetic relationships within the *Laudakia caucasia* species group on the Iranian Plateau were investigated using 1708 aligned bases of mitochondrial DNA sequence from the genes encoding ND1 (subunit one of NADH dehydrogenase), tRNA^{Gln}, tRNA^{Ile}, tRNA^{Met}, ND2, tRNA^{Trp}, tRNA^{Ala}, tRNA^{Asn}, tRNA^{Cys}, tRNA^{Tyr}, and COI (subunit I of cytochrome *c* oxidase). The aligned sequences contain 207 phylogenetically informative characters. Three hypotheses for historical fragmentation of *Laudakia* populations on the Iranian Plateau were tested. In two hypotheses, fragmentation of populations is suggested to have proceeded along continuous mountain belts that surround the Iranian Plateau. In another hypothesis, fragmentation is suggested to have resulted from a north–south split caused by uplifting of the Zagros Mountains in the late Miocene or early Pliocene [5–10 MYBP (million years before present)]. The shortest tree suggests the latter hypothesis, and statistical tests reject the other two hypotheses. The phylogenetic tree is exceptional in that every branch is well supported. Geologic history provides dates for most branches of the tree. A plot of DNA substitutions against dates from geologic history refines the date for the north–south split across the Iranian Plateau to 9 MYBP (late Miocene). The rate of evolution for this segment of mtDNA is 0.65% (0.61–0.70%) change per lineage per million years. A hypothesis of area relationships for the biota of the Iranian Plateau is generated from the phylogenetic tree. © 1998 Academic Press

Key Words: Reptilia; Sauria; Iguania; Agamidae; historical biogeography; mitochondrial DNA; phylogenetics; Asia; Armenia; Iran; Russia; Tajikistan; Turkmenistan.

INTRODUCTION

Three species of the *Laudakia caucasia* species group occur on the Iranian Plateau (Fig. 1). *L. caucasia* occurs

continuously from the Caucasus Mountains through the Elborz Mountains of northern Iran to the western Kopet-Dagh Mountains of southern Turkmenistan. Geographically isolated populations attributed to *L. caucasia* are found in the Little and Big Balkhan mountains north of the Kopet-Dagh Mountains in southern Turkmenistan. *Laudakia erythrogastra* occurs in the eastern Kopet-Dagh Mountains and the Badkyz Plateau of southern Turkmenistan and northeastern Iran. *Laudakia microlepis* is found in the Zagros Mountains and Khurasan Hills of southern and eastern Iran.

Two subspecies of *L. caucasia* are currently recognized, *L. c. caucasia* and *L. c. triannulata* (Ananjeva and Atayev, 1984; Anan'eva and Tuniev, 1994). *L. c. triannulata* is geographically isolated from *L. c. caucasia* and occurs in eroded sand canyons west of the Kopet-Dagh Mountains in the Caspian Sea floodplain. Two subspecies of *L. erythrogastra* are recognized; *L. e. nurgeldievi* occurs in the eastern Kopet-Dagh Mountains, and *L. e. erythrogastra* on the Badkyz Plateau (Anan'eva and Tuniev, 1994; Tuniyev *et al.*, 1991).

Populations of *Laudakia* are found in rocky mountain habitats and eroded sand canyons in floodplains adjacent to mountains, but they are absent from flat gravel and sandy deserts, which serve as barriers to dispersal. The mountain belts surrounding the Iranian Plateau are continuous; from the northeast they extend from the Badkyz Plateau and the Kopet-Dagh Mountains of Turkmenistan to the Lesser Caucasus Mountains in the northwestern portion of the Iranian Plateau and to the Zagros Mountains of southern Iran. In the central and eastern portion of the Iranian Plateau, the flat gravel and sandy desert regions of the Dasht-i-Lut and Dasht-i-Kavir have no *Laudakia* habitat, providing a barrier to dispersal. In the northeastern portion of the Iranian Plateau, the Dasht-i-Kavir connects with the Siestan and Helmand basins of extreme eastern Iran and Afghanistan and provides a low-elevation barrier of flat gravel and sandy desert. The mountains on the southern and northern sides of the

¹ To whom correspondence should be addressed. Fax: (314) 935-4432. E-mail: Larson@wustlb.wustl.edu.



FIG. 1. Map of the Middle East showing localities from which *Laudakia* populations were sampled. The two outgroup taxa, *L. himalayana* and *L. lehmanni*, are from Tajikistan (labeled "Pamir"). *Laudakia erythrogastra* and *L. caucasica* populations are numbered and are mostly from Turkmenistan. The *L. erythrogastra* (closed circle) population 1 is from the Badkyz Plateau and population 2 is from the eastern Kopet-Dagh of Turkmenistan. Population 1 is recognized as *L. e. erythrogastra*, whereas population 2 is considered *L. e. nurgeldievi*. The *L. caucasica* (closed square) populations 1 and 2 are from the central and western Kopet-Dagh of Turkmenistan, respectively. Population 3 is from the Caspian Sea floodplain in Turkmenistan and is recognized as *L. c. triannulata*. Populations 4 and 5 are from the Little and Big Balkhan mountains respectively, in Turkmenistan. Population 6 is from Armenia and 7 is from Dagestan, Russia. See Materials and Methods for exact localities.

Iranian Plateau are connected to the Pamir and Hindu Kush mountains of Pakistan, Afghanistan, and Tajikistan where related *Laudakia* taxa occur (i.e., *L. himalayana* and *L. lehmanni*).

This topographic pattern suggests that divergence of populations and species may have occurred sequentially along this continuous mountain belt. A phylogenetic tree would be expected to show sequential branching connecting populations distributed along this mountain chain (Fig. 2, hypotheses 1 and 2). Alternatively, an older separation of populations could have taken place when the Zagros Mountains of southern Iran and the more northern Kopet-Dagh and Lesser Caucasus mountains were beginning to uplift in the late Miocene to early Pliocene (5–10 MYBP, Fig. 2, hypothesis 3). These hypotheses are testable contingent upon a reliable phylogenetic estimate.

To investigate the phylogenetic relationships of the *L. caucasica* species group, over 1700 bases of mitochondrial DNA were sequenced from 12 populations representing all species and subspecies of the *L. caucasica* species group and two outgroup taxa. The two outgroup taxa, *L. himalayana* and *L. lehmanni*, are from the Pamir Mountains near the connection with the Hindu Kush Mountains in Tajikistan. These taxa were selected based on a phylogenetic study of the families Agamidae and Chamaeleonidae using the same mitochondrial-DNA region reported here (unpublished data).

One population of *L. microlepis* was sampled from the Zagros Mountains of southern Iran. Two populations of *L. erythrogastra* were sampled, *L. e. nurgeldievi* from the eastern Kopet-Dagh Mountains (Tuniyev *et al.*, 1991) and *L. e. erythrogastra* from the Badkyz Plateau, both in Turkmenistan. Seven populations of *L.*

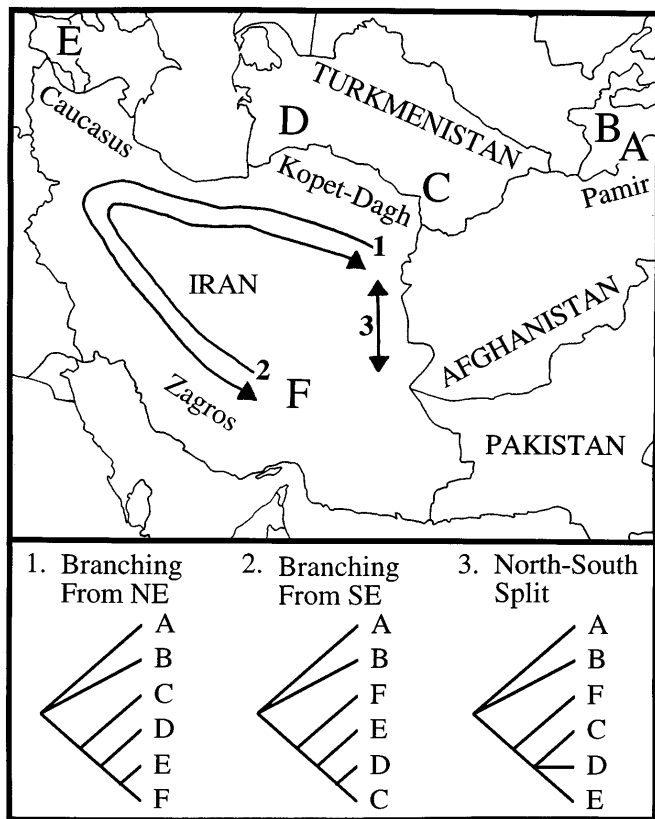


FIG. 2. Hypotheses for fragmentation of *Laudakia* populations. Outgroup taxa are from the high Pamir (A, *L. himalayana*) and the low Pamir (B, *L. lehmanni*). (1) Sequential branching occurs from the northeast around the continuous mountain belts of the Iranian Plateau [(C) Badkyz Plateau and eastern Kopet-Dagh to (D) western Kopet-Dagh and Balkhans to (E) Caucasus and (F) Zagros]. (2) Sequential branching occurs from the southeast around the continuous mountain belts of the Iranian Plateau [(F) Zagros to (E) Caucasus, to (D) western Kopet-Dagh and Balkhans to (C) eastern Kopet-Dagh and Badkyz Plateau]. (3) Branching pattern expected from a late Miocene to early Pliocene split north-south across the Iranian Plateau. The Zagros (F) is expected to be the sister taxon to all northern populations (C-E). Note that the topology expected in the second scenario, sequential branching along mountain belts from the southeast, is one of three topologies compatible with the third hypothesis, a north-south split. The topology of the second scenario is compatible with a north-south split only if the split occurs in the western portion of the Iranian Plateau. The two other topologies are unique and suggest a north-south split occurring in either the eastern (A, B, (C, (D, E))) or central (A, B, (D, (C, E))) portions of the Iranian Plateau.

caucasica were sampled. Populations sampled in Turkmenistan were from the central and western Kopet-Dagh Mountains (two populations, Fyrusa and Temen Spring, respectively), the Big Balkhan Mountains, the Little Balkhan Mountains, and the Caspian Sea floodplain. All populations in Turkmenistan are recognized as *L. c. caucasica* except the one from the Caspian Sea floodplain which is considered *L. c. triannulata* (Ananjeva and Atayev, 1984). In the Caucasus Mountains, two populations of *L. c. caucasica* were sampled, one

from Dagestan, Russia (in the Greater Caucasus Mountains), and the other from Armenia (in the Lesser Caucasus Mountains), just north of Iran.

This sampling allows a hypothesis of fragmentation along the Iranian Plateau mountain belts to be tested against the alternative hypothesis of a north-south splitting event occurring in the late Miocene to early Pliocene. The phylogenetic tree is expected to root in the east where the two outgroup taxa occur, and successive branching events should continue west (Fig. 2). Because two species of the *L. caucasica* species group, *L. erythrogastra* and *L. microlepis*, occur in the eastern portion of the Iranian Plateau, two scenarios may be tested for fragmentation occurring along continuous mountain belts. If sequential branching occurs from the northeast, *L. erythrogastra* should be in a basal position, with successive branching occurring to the west and south. In this case, populations from the western Kopet-Dagh and Balkhan mountains (*L. caucasica*) should be the sister taxon to a clade comprising populations from the Caucasus (*L. caucasica*) and Zagros mountains (*L. microlepis*), (Fig. 2, hypothesis 1). Alternatively, if sequential branching occurs from the southeast, *L. microlepis* from the Zagros Mountains should be in a basal position. In this case, the northwestern populations from the Caucasus Mountains (*L. caucasica*) should be the sister taxon to a clade comprising all populations to the east from Turkmenistan (*L. caucasica* western Kopet-Dagh and Balkhans, *L. erythrogastra* eastern Kopet-Dagh and Badkyz), (Fig. 2, hypothesis 2). In both scenarios *L. caucasica* would not be monophyletic. Interestingly, *L. microlepis* is often considered a subspecies of *L. caucasica*, suggesting the first scenario (see Anderson, 1974).

Alternatively, if a north-south split in the late Miocene to early Pliocene (5-10 MYBP) is responsible for fragmentation of northern and southern populations on the Iranian Plateau, then *L. microlepis*, occurring in the more southern Zagros Mountains, is expected to be the sister taxon to all northern populations of the *L. caucasica* species group (*L. caucasica* and *L. erythrogastra*), (hypothesis 3, Fig. 2). Specifically, three possible topologies that show alternative branching patterns of northern taxa are compatible with a north-south split. If this splitting event occurred in the west, the expected topology would be identical to that predicted by a hypothesis of sequential branching starting in the southeast and proceeding around the Iranian Plateau (hypothesis 2, Fig. 2). Hence, if the data support this topology, the hypothesis of a north-south split could not be distinguished empirically from one of sequential branching along continuous mountain belts. Alternatively, if this north-south split occurred in the eastern or central portions of the Iranian Plateau, the expected topology would differ from that of hypotheses 1 and 2 in Fig. 2. If the data reject hypotheses 1 and 2 (Fig. 2), a north-south split is favored over sequential

branching occurring along continuous mountain belts. See Fig. 2 for details of these hypotheses.

MATERIALS AND METHODS

Specimen Information

Museum numbers and localities for voucher specimens from which DNA was extracted and GenBank Accession numbers are presented below. Acronyms are CAS for California Academy of Sciences, San Francisco; MVZ for Museum of Vertebrate Zoology, University of California at Berkeley; and GNM.RE.ex for the Göteborg Natural History Museum Reptilia Exotica, Göteborg, Sweden. The specimen deposited in GNM.RE.ex is followed by a dash P which corresponds to the field number of the fifth author. Population numbers for *L. caucasia* and *L. erythrogastra* correspond to those in Fig. 1.

Laudakia himalayana: CAS183016, AF028676, Tajikistan, 5 km east of the road to Dzhirgatal' (39° 13' N 71° 12' E) on the Djalar to Djalzan Rd. *Laudakia lehmanni*: CAS183009, AF028677, Tajikistan, Okbulok Kishlak, Aktau Mountain Ridge, approx. 50 km SW of Dushanbe. *Laudakia microlepis*: GNM.RE.ex.-P120, AF028678, Iran, Kerman Province, Khaneh-ye Sorkh Pass (29° 49' N 56° 06' E), 65 km NE of Sirjan on the road to Kerman. *Laudakia erythrogastra*: (1) CAS182954, AF028679, Turkmenistan, Badkyz Plateau, near Pul-i-khatun (39° 59' N 64° 38' E); (2) CAS184400, AF028680, Turkmenistan, 37° 12' N 59° 33' E, within 2 km NE and NW of Khiveabad, along the Turkmenistan–Iran control border. *Laudakia caucasia*: (1) CAS185010, AF028681, Turkmenistan, 38° 01' N 58° 02' E, Lower Chuli, 12 km NNW (airline) of Fyrusa; (2) CAS184770, AF028682, Turkmenistan, 39° 06' N 55° 08' E, vicinity of Temen Spring, 2.5 km west of Danata (39° 07' N 55° 08' E); (3) CAS184650, AF028683, Turkmenistan, 39° 10' N 54° 44' E, 14.2 km SW of Madau; (4) CAS184852, AF028684, Turkmenistan, 39° 14' N 54° 58' E, Chalsu Valley, base of the Maly (Little) Balkhan Mountains, 36 km west of the 2-km-long road south to Kazandjik; (5) CAS184561, AF028685, 39° 45' N 54° 33' E, Turkmenistan, foothills adjacent to the northern slope of the Bolshoy (Big) Balkhan Mountains, 12 km ESE of Akrobat (39° 45' N 54° 22' E); (6) CAS194304, AF028686, Armenia, Lake Seivan (40° 30' N 45° 30' E); (7) CAS182808, AF028687, Russia, Dagestan Autonomous Republic, vicinity of Sary Kum Sand Dunes, approx. 12 km west (airline) of Makhachkala (42° 58' N 47° 30' E).

Laboratory Protocols

Genomic DNA was extracted from liver using the Qiagen QIAamp tissue kit. Amplification of genomic DNA was conducted using a denaturation at 94°C for 35 s, annealing at 50°C for 35 s, and extension at 70°C for 150 s with 4 s added to the extension per cycle for 30 cycles. Negative controls were run for all amplifications. Amplified products were purified on 2.5% Nusieve GTG agarose gels and reamplified under similar condi-

tions. Reamplified double-stranded products were purified on 2.5% acrylamide gels (Maniatis *et al.*, 1982). Template DNA was eluted from acrylamide passively over 3 days with Maniatis elution buffer (Maniatis *et al.*, 1982). Cycle-sequencing reactions were run using the Promega fmol DNA-sequencing system with a denaturation at 95°C for 35 s, annealing at 53–60°C for 35 s, and extension at 70°C for 1 min for 30 cycles. Sequencing reactions were run on Long Ranger sequencing gels for 5–12 h at 38–40°C.

Amplifications from genomic DNA were done using different primer combinations (Table 1): (1) L4160-H5934, (2) L4178a-H4980 and L4437-H5934, or (3) L3878-H4980 and L4437-H5934. *L. himalayana* would not work for primers H5934 or H5937a and was amplified using L4178b-H4980, L4437-H5617a, and L4831-H6564. Sequences were acquired using primers listed in Table 1. *L. himalayana* was the only sample sequenced with H5937b. Primer numbers refer to the 3' end on the human mitochondrial genome (Anderson *et al.*, 1981), where L and H correspond to light and heavy strands, respectively.

Sequence Alignment

Reported sequences are presented in Fig. 3 and correspond to positions 4180 to 5936 on the human mitochondrial genome (Anderson *et al.*, 1981). This sequence contains the genes encoding ND1 (subunit one of NADH dehydrogenase), tRNA^{Gln}, tRNA^{Ile}, tRNA^{Met}, ND2, tRNA^{Trp}, tRNA^{Ala}, tRNA^{Asn}, tRNA^{Cys}, tRNA^{Tyr}, and COI (subunit I of cytochrome *c* oxidase). No length variation was found in protein-coding genes, making alignment straightforward. Protein-coding sequences were translated to amino acids using MacClade (Maddison and Maddison, 1992) for confirmation of alignment.

Transfer-RNA secondary structure was determined manually using the criteria of Kumazawa and Nishida (1993) to ensure proper alignment (Macey and Verma, 1997). In two tRNA stems, a deletion appears to have occurred in the stem adjacent to a loop, and the bases at the end of the stem do not pair. In the T Ψ C stems of the tRNA^{Ile} and tRNA^{Cys} genes, gaps were placed in the stem to align loop bases. This alignment is conservative because these positions are invariant in our alignment.

Two tRNA loops were excluded. The 14 positions in the T Ψ C loop of the tRNA^{Trp} gene and the dihydrouridine (D)-arm replacement loop of the tRNA^{Cys} gene (Macey *et al.*, 1997b) were unalignable and not included in the analysis. Note that in the alignment presented in Fig. 3, the 7 positions in the D-arm replacement loop of the tRNA^{Cys} gene contain no phylogenetically informative characters. Of the 1722 aligned positions, 1708 were used in the phylogenetic analysis. Transfer-RNA genes that encode tRNAs with D-arm replacement loops are subject to stem realignments and shifts in bases from one stem to another, making homology of bases difficult to assess (Macey *et al.*, 1997b). The

TABLE 1
Primers Used in This Study

Human position	Gene	Sequence	Reference
L3878	ND1	5'-GCCCCATTTGACCTCACAGAAGG-3'	Macey <i>et al.</i> (1998)
L4160	ND1	5'-CGATTCCGATATGACCARCT-3'	Kumazawa and Nishida (1993)
L4178a	ND1	5'-CARCTWATACACYTACTATGAAA-3'	Macey <i>et al.</i> (1997a)
L4178b	ND1	5'-CAACTAATACACCTACTATGAAA-3'	Macey <i>et al.</i> (1997a)
H4419	tRNA ^{Met}	5'-GGTATGAGCCCCAATTGCTT-3'	Macey <i>et al.</i> (1997a)
L4437	tRNA ^{Met}	5'-AAGCAGTTGGGCCCATRCC-3'	Macey <i>et al.</i> (1997c)
L4831	ND2	5'-TGACTTCCAGAAGTAATACAAGG-3'	Macey <i>et al.</i> (1997a)
H4980	ND2	5'-ATTTTCGTAGTTGGGTTTGRRT-3'	Macey <i>et al.</i> (1997a)
L5002	ND2	5'-AACCAAACCCAACCTACGAAAAAT-3'	Macey <i>et al.</i> (1997a)
H5617a	tRNA ^{Ala}	5'-AAAATRTCTGRGTTGCATTCAG-3'	Macey <i>et al.</i> (1997a)
H5617b	tRNA ^{Ala}	5'-AAAAGTGTCTGAGTTGCATTCAG-3'	Macey <i>et al.</i> (1997a)
L5638	tRNA ^{Ala}	5'-CTGAATGCAACYCAGAYATTTT-3'	Macey <i>et al.</i> (1997a)
H5934	COI	5'-AGRGTGCCAATGTCTTTTGTGRTT-3'	Macey <i>et al.</i> (1997a)
H5937a	COI	5'-GTGCCAATGTCTTTGTG-3'	Macey <i>et al.</i> (1997a)
H5937b	COI	5'-GTGCCAATATCTTTRTG-3'	Kumazawa and Nishida (1993)
H6564	COI	5'-GGTCTCCTCCTCCAGCTGGGTC-3'	This study

Note. Primers are designated by their 3' ends which correspond to the position in the human mitochondrial genome (Anderson *et al.*, 1981) by convention. H and L designate heavy-strand and light-strand primers, respectively. Positions with mixed bases are labeled with the standard one-letter code: R = G or A, Y = C or T, W = A or T.

tRNA^{Cys} gene sequences reported here all appear to encode tRNAs with secondary structures composed of homologous bases, allowing proper alignment.

Phylogenetic Analysis

Phylogenetic trees were estimated using PAUP (Swofford, 1993) with branch-and-bound searches. Bootstrap resampling was applied to assess support for individual nodes with 1000 bootstrap replicates using branch-and-bound searches. Decay indices (=“branch support” of Bremer, 1994) were calculated for all internal branches of the tree using branch-and-bound searches that retained suboptimal trees.

Templeton's (1983) test, conducted as a two-tailed Wilcoxon signed-ranks test (Felsenstein, 1985), was applied to examine statistical significance of the shortest trees relative to alternative hypotheses. This test asks whether the most parsimonious tree is significantly shorter than an alternative or whether their differences in length can be attributed to chance alone (Larson, 1994). The test statistic, T_s , was compared with critical values for the Wilcoxon rank sum in Table B.11 of Zar (1984).

Alternative biogeographic hypotheses were tested

using the most parsimonious phylogenetic topologies compatible with them. To find the most parsimonious tree(s) compatible with a particular biogeographic hypothesis, phylogenetic topologies were constrained using MacClade (Maddison and Maddison, 1992) and analyzed using PAUP (Swofford, 1993) with a branch-and-bound search. Statistical tests were conducted using the “compare trees” option of MacClade (Maddison and Maddison, 1992).

Kitch and Fitch trees were generated using PHYLIP (Felsenstein, 1995) and compared to determine whether our sequences have evolved in a clock-like fashion.

RESULTS

Sequences ranging in size from 1710 to 1716 bases of mitochondrial DNA for 12 samples of *Laudakia* are presented as 1722 aligned positions in Fig. 3.

Authentic Mitochondrial DNA

Several observations suggest that the DNA sequences analyzed here are from the mitochondrial genome and do not represent nuclear-integrated copies of mitochondrial genes (see Zhang and Hewitt, 1996).

FIG. 3. Alignment of *Laudakia* sequences analyzed for phylogenetic inference. Positions 321–1280 from the ND2 gene are not shown because they contain no length variation, giving an unambiguous alignment. Sequences excluded from phylogenetic analyses are designated above with doubly underlined headings, “Exclude” and “D-Loop.” The D-arm replacement loop of the tRNA^{Cys} gene is designated “D-Loop” and the loop sequence is singly underlined. The stem-and-loop structures between the tRNA^{Asn} and tRNA^{Cys} genes have the heading and stem regions of the sequence singly underlined. Stop codons for the ND1 and ND2 genes as well as start codons for the ND2 and COI genes are singly underlined. Sequences are presented as light-strand sequence and tRNA secondary structure is designated above the sequence. Stems are indicated by arrows in the direction encoded: AA, amino acid-acceptor stem; D, dihydrouridine stem; AC, anticodon stem; T, T_ψC stem. The tRNA anticodons are designated COD. Asterisks indicate the unpaired 3' tRNA position 73. Periods represent bases located outside stem regions; “1” depicts the first codon position of protein-coding sequences.

Protein-coding genes do not have premature stop codons, suggesting that these sequences represent functional copies that encode a protein. Transfer-RNA genes appear to code for tRNAs with stable secondary structures, indicating functional genes. The presence of strand bias further supports our conclusion that the 12 DNA sequences reported here are from the mitochondrial genome. The sequences reported here show strong strand bias against guanine on the light strand (G = 11.1–11.8%, A = 37.8–39.0%, T = 22.9–23.5%, and C = 26.4–27.5%), which is characteristic of the mitochondrial genome but not the nuclear genome. Therefore, we interpret these sequences as authentic mitochondrial DNA.

Genomic Organization, Origin for Light-Strand Replication, and tRNA^{Cys}

Three structural features of the mitochondrial genome (genomic organization, origin for light-strand replication, and secondary structure of tRNA^{Cys}) show derived states in acrodont lizards (Macey *et al.*, 1997a,b,c). Most vertebrates have a mitochondrial gene order of ND1, tRNA^{Ile}, tRNA^{Gln}, tRNA^{Met}, ND2, tRNA^{Trp}, tRNA^{Ala}, tRNA^{Asn}, O_L (origin for light-strand replication), tRNA^{Cys}, tRNA^{Tyr}, and COI. In acrodont lizards the tRNA^{Ile} and tRNA^{Gln} genes are switched in order (Fig. 3) and the O_L appears to be absent (Fig. 4). Some acrodont lizards (*Uromastix* and *Physignathus*, Macey *et al.*, 1997a,c) lack any sequence between the tRNA^{Asn} and tRNA^{Cys} genes, where O_L is typically located in vertebrates. Another genus (*Phrynocephalus*, Macey *et al.*, 1997c) has a sequence that cannot form a stable secondary structure typical for O_L among vertebrates. Other genera (*Chamaeleo* and *Leiolepis*, Macey *et al.*, 1997c) contain stem-and-loop structures in the typical vertebrate position for O_L between the tRNA^{Asn} and tRNA^{Cys} genes, but these sequences do not have the functional characteristics of O_L identified in studies of mammalian mitochondrial replication (Brennicke and Clayton, 1981; Hixson *et al.*, 1986). *Laudakia* have stem-and-loop structures in the typical vertebrate position for O_L between the tRNA^{Asn} and tRNA^{Cys} genes, but they do not resemble sequences reported from other acrodont lizards. They also lack functional characteristics required for replication in mammals (Fig. 4). We therefore interpret these sequences as nonfunctional.

The tRNA^{Cys} gene of acrodont lizards encodes a tRNA that lacks a D-stem and instead contains a D-arm replacement loop (Fig. 3, Macey *et al.*, 1997b). This loop is highly variable (Fig. 3).

The sequences reported here provide further evidence that shifts in gene order, loss of a recognizable origin for light-strand replication between the tRNA^{Asn} and tRNA^{Cys} genes, and changes in secondary structure of tRNA^{Cys} are not subject to evolutionary reversal (Macey *et al.*, 1997a,b,c).

Genic Variation

Different levels of variation were observed among the three protein-coding genes, eight tRNA-coding genes, and

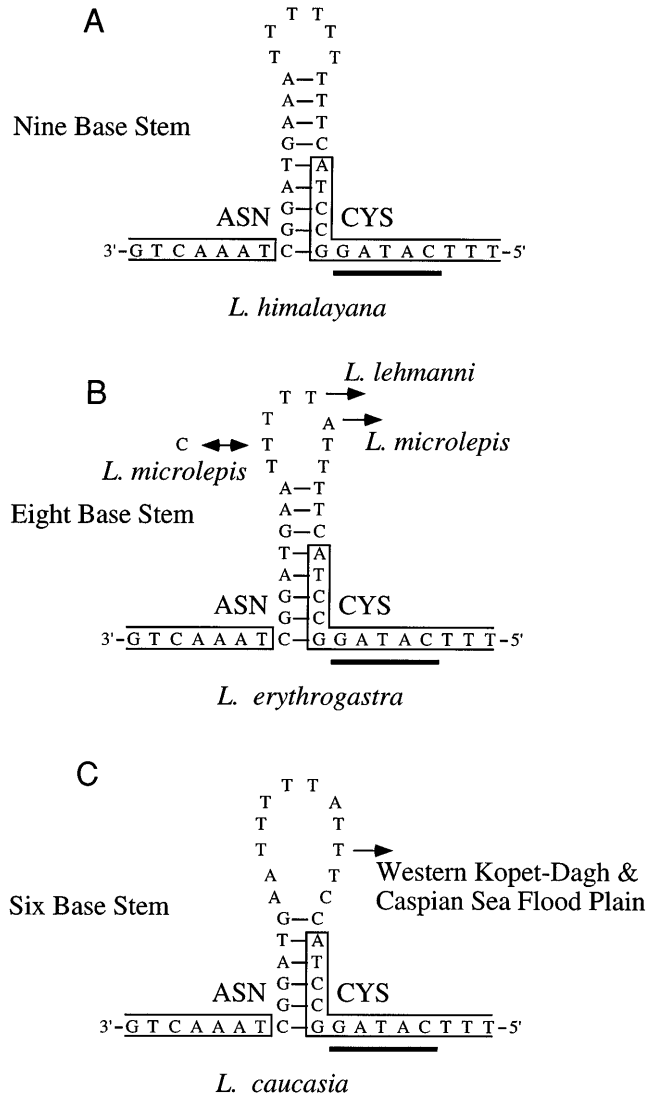


FIG. 4. Stem-and-loop structures between the tRNA^{Asn} and tRNA^{Cys} genes observed in *Laudakia*. Nucleotide deletions in taxa are denoted with an arrow, and substitutions are depicted with a double arrow. Note that the stem varies in length among taxa. None of the stems contain the heavy-strand template sequence 3'-GCC-5' identified as the point of light-strand elongation in mouse (Brennicke and Clayton, 1981). The bases underlined represent the position where the heavy-strand sequence 3'-GGCCG-5' required for *in vitro* light-strand replication in humans (Hixson *et al.*, 1986) should be located. This sequence varies in reptiles and should consist of a 3'-GBCCB-5' sequence (B = G, C, or T) (Macey *et al.*, 1997a,c), but is not present in *Laudakia*.

two noncoding regions (Table 2). Most of the variation and the phylogenetically informative sites were from protein-coding regions. Only 74 variable and 36 phylogenetically informative sites were from tRNA genes and noncoding regions. Of the 171 phylogenetically informative characters from protein-coding regions, 111 are from third positions of codons. Third-position sites account for over half of the phylogenetically informative sites in the total data set. Only 17 phylogenetically informative sites occur in regions

TABLE 2

Distribution of Phylogenetically Informative (Parsimony Criterion) and Variable Positions

	ND1 codon positions			tRNA ^{Gln}		Noncoding region 1 ^a	tRNA ^{Ile}		tRNA ^{Met}	
	1st	2nd	3rd	Stem	Nonstem		Stem	Nonstem	Stem	Nonstem
Informative sites	5	3	12	2	—	5	1	3	—	2
Variable sites	8	4	17	5	8	6	2	6	3	4
	ND2 codon positions			tRNA ^{Trp} ^b		tRNA ^{Ala}		tRNA ^{Asn}		Noncoding region 2 ^a
	1st	2nd	3rd	Stem	Nonstem	Stem	Nonstem	Stem	Nonstem	
Informative sites	40	12	95	1	2	2	4	6	1	1
Variable sites	81	42	178	2	3	2	5	8	1	4
	tRNA ^{Cys} ^b			tRNA ^{Tyr}		COI codon positions				
	Stem	Nonstem		Stem	Nonstem	1st	2nd	3rd		
Informative sites	4	1		1	—	—	—	—		4
Variable sites	6	1		5	3	1	1			6
Total	Protein coding codon positions			tRNA		Noncoding regions	All aligned sequence			
	1st	2nd	3rd	Stem	Nonstem					
Informative sites	45	15	111	17	13	6	207			
Variable sites	90	47	201	33	31	10	412			

^a Noncoding region 1 is between the tRNA^{Gln} and tRNA^{Ile} genes, and noncoding region 2 is between the tRNA^{Asn} and tRNA^{Cys} genes.

^b Not including excluded positions, which are the TΨC-loop of the tRNA^{Trp} gene and the D-arm replacement loop of the tRNA^{Cys} gene.

encoding stems of tRNAs, suggesting that compensatory substitutions do not compromise the phylogenetic analysis.

Phylogenetic Relationships

A single tree was produced from the parsimony analysis of the 1708 aligned DNA sequences containing 207 phylogenetically informative base positions (Fig. 5, Table 2). Phylogenetic relationships are well resolved for all nodes of the tree. Monophyly of the *L. caucasia* species group is strongly supported by a bootstrap value of 98% and a decay index of 13. The more northern *L. erythrogastra* and *L. caucasia* are each monophyletic and show a branching pattern that goes from east to west.

The more southern *L. microlepis* appears as the sister taxon to an extremely well supported (bootstrap 100%, decay index 55) clade containing all *L. erythrogastra* and *L. caucasia* populations. Support for monophyly of *L. erythrogastra* populations is strong (bootstrap 100%, decay index 21). Monophyly of *L. caucasia* populations receives strong support from a bootstrap value of 100% and a decay index of 14. Three clades are distinguished within *L. caucasia*. Two groups in Turkmenistan are monophyletic (bootstrap 100%, decay index 11). The populations in the central and western Kopet-Dagh (Fyrusa and Temen Spring, respectively) form a monophyletic group with *L. c. triannulata* from the adjacent Caspian Sea floodplain (bootstrap 100%, decay index 11). The Temen Spring population in the western Kopet-Dagh is the sister population to the

geographically adjacent *L. c. triannulata* population (bootstrap 100%, decay index 5) occurring on the Caspian Sea floodplain. The other clade identified in Turkmenistan occurs in the Little Balkhan and Big Balkhan mountains and is the sister taxon to populations from the western Kopet-Dagh and the Caspian Sea floodplain. Monophyly of the two Balkhan mountains populations is supported by a bootstrap value of 99% and a decay index of 4. Monophyly of *L. caucasia* populations from the Caucasus Mountains, Armenia and Dagestan, is well supported (bootstrap 100%, decay index 14).

To test hypotheses of fragmentation along continuous mountain belts of the Iranian Plateau versus the north-south split across the Iranian Plateau, Templeton's (1983) test was applied. The shortest alternative tree constrained to show successive branching patterns around the Iranian Plateau from the northeast (Appendix; hypothesis 1 in Fig. 2) differed from the overall shortest tree only in the placement of *L. microlepis* as the sister taxon to the *L. caucasia* populations from the Caucasus Mountains (Armenia and Dagestan). When the overall shortest tree was compared to this alternative tree showing a sequential branching pattern from the northeast (hypothesis 1 in Fig. 2), this alternative was rejected in favor of the overall shortest tree ($n = 77$, $T_s = 78$, $P < 0.001$). The shortest alternative tree constrained to show successive branching patterns around the Iranian Plateau from the southeast (Appendix;

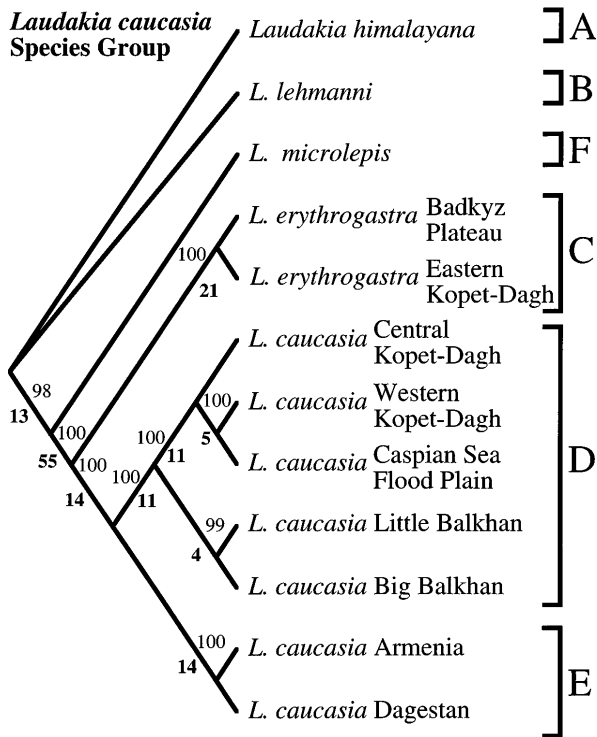


FIG. 5. The single most parsimonious tree found from a branch-and-bound search. The tree has a length of 549 steps and a consistency index of 0.865. Bootstrap values are presented above branches and decay indices are shown in bold below branches. Note that all internal nodes are well supported. Populations are labeled with letters as in Fig. 2. A branching pattern is observed that is compatible only with hypothesis 3 in Fig. 2, a north-south split in the eastern portion of the Iranian Plateau.

hypothesis 2 in Fig. 2) differed from the overall shortest tree only in the placement of *L. erythrogastra* populations as the sister taxon to the *L. caucasia* populations from Turkmenistan (central and western Kopet-Dagh, Caspian Sea floodplain, Little Balkhan, and Big

Balkhan). When the overall shortest tree was compared to this alternative tree showing a sequential branching pattern from a southeastern root (hypothesis 2 in Fig. 2), this alternative was rejected in favor of the overall shortest tree ($n = 17$, $T_s = 9$, $P < 0.001$). The overall shortest tree is consistent with a late Miocene to early Pliocene (5–10 MYBP) split that separated populations in the northeastern and southeastern portions of the Iranian Plateau.

Phylogeny, Nucleotide Substitutions, and Taxonomy

The phylogenetic hypothesis placed *L. c. triannulata* within *L. c. caucasia*. Only four nucleotide substitutions occur between *L. c. triannulata* (Caspian Sea floodplain) and the nearest *L. c. caucasia* population (Temen Spring in the western Kopet-Dagh). We suggest that recognition of subspecies be discontinued for *L. caucasia* to avoid recognizing the paraphyletic *L. c. caucasia*. *L. caucasia* is nonetheless a phylogenetically fragmented taxon; our sinking of the subspecies does not imply genetic homogeneity among populations.

The two populations of *L. erythrogastra* examined are considered distinct subspecies. Only 11 nucleotide substitutions were found between *L. e. erythrogastra* from the Badkyz Plateau and *L. e. nurgeldievi* occurring in the eastern Kopet-Dagh. This difference is less than that observed between *L. caucasia* populations in the Kopet-Dagh (14 substitutions). We therefore suggest that recognition of subspecies be discontinued for *L. erythrogastra*.

DISCUSSION

The testing of alternative hypotheses for fragmentation of populations on the Iranian Plateau revealed a north-south split for *Laudakia*. Alternative hypotheses that suggest sequential fragmentation along con-

TABLE 3

Pairwise Comparisons of DNA Sequences among Populations of the *L. caucasia* Species Group and Outgroup Taxa

	1	2	3	4	5	6	7	8	9	10	11	12
1. <i>L. himalayana</i>	—	193	196	207	206	201	200	209	207	205	203	204
2. <i>L. lehmanni</i>	11.3%	—	214	230	228	239	238	238	235	230	234	235
3. <i>L. microlepis</i>	11.5%	12.5%	—	192	189	195	196	200	200	195	199	199
4. <i>L. erythrogastra</i> Badkyz Plateau	12.1%	13.5%	11.2%	—	11	71	76	86	86	83	74	75
5. <i>L. erythrogastra</i> E. Kopet-Dagh	12.1%	13.3%	11.1%	0.6%	—	76	81	91	91	88	77	78
6. <i>L. caucasia</i> Dagestan	11.8%	14.0%	11.4%	4.2%	4.4%	—	8	53	53	54	39	40
7. <i>L. caucasia</i> Armenia	11.7%	13.9%	11.5%	4.4%	4.7%	0.5%	—	59	59	59	45	46
8. <i>L. caucasia</i> Caspian Sea plain	12.2%	13.9%	11.7%	5.0%	5.3%	3.1%	3.5%	—	4	14	25	26
9. <i>L. caucasia</i> W. Kopet-Dagh	12.1%	13.8%	11.7%	5.0%	5.3%	3.1%	3.5%	0.2%	—	14	27	28
10. <i>L. caucasia</i> C. Kopet-Dagh	12.0%	13.5%	11.4%	4.9%	5.2%	3.2%	3.5%	0.8%	0.8%	—	25	26
11. <i>L. caucasia</i> Little Balkhan	11.9%	13.7%	11.7%	4.3%	4.5%	2.3%	2.6%	1.5%	1.6%	1.5%	—	1
12. <i>L. caucasia</i> Big Balkhan	11.9%	13.8%	11.7%	4.4%	4.6%	2.3%	2.7%	1.5%	1.6%	1.5%	0.01%	—

Note. The number of base substitutions between sequences is shown above the diagonal and the percentage of sequence divergence is shown below the diagonal.

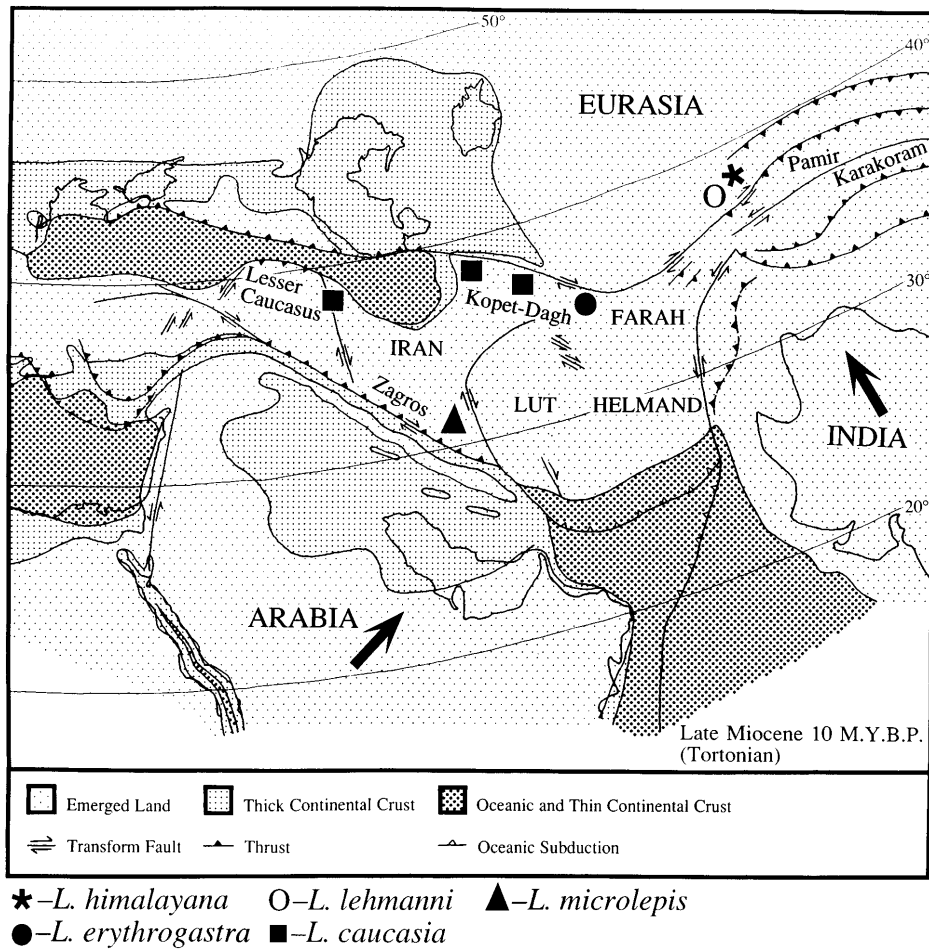


FIG. 6. Tectonic setting for the formation of mountain belts around the Iranian Plateau and the position of *Laudakia* species. The map is after Dercourte *et al.* (1986) and uplifting in the Pamir and Karakoram mountains is schematic after Tapponier *et al.* (1981). Tectonic processes depicted here continue today. During the late Miocene (10 MYBP, Tortonian), India wedged deeply into Eurasia, and Arabia began indentation into Iran (composed of Cimmerian Plates). The Pamir Mountains, where the two outgroup taxa (*L. himalayana* and *L. lehmanni*) occur, were experiencing intense uplifting during the late Miocene (10 MYBP). The indentation of Arabia into Iran in the late Miocene (10 MYBP) began the formation of the Zagros Mountains in the southern part of the Iranian Plateau where *L. microlepis* occurs. In the northern part of the Iranian Plateau, the Lesser Caucasus Mountains and Kopet-Dagh, where *L. caucasia* and *L. erythrogastra* occur, began uplifting in the early Pliocene (5 MYBP). Plates are labeled in capital letters and Cimmerian Plates are Iran, Lut, Farah, and Helmand. Note that the indentations of both India and Arabia are compressing the Cimmerian Plates and causing intense mountain building along paleosutures of these plates.

tinuous mountain belts around the Iranian Plateau were rejected.

Geologic History and Fragmentation of Laudakia Populations

Prior to formation of the present Eurasian continent, an extremely complex history of microcontinental plate accretions occurred. These early plate accretions created sutures that were later reactivated as strike-slip (transform) faults in the Tertiary by the Indian and Arabian collisions. The positioning of these sutures created a setting for future fault movements that shaped the topography of the Iranian Plateau. We review the pre-Eocene and subsequent Tertiary events that helped shape the present Asian topography. Dates

are presented as millions of years before the present (MYBP).

A complex series of events occurred with the successive accretion of blocks to the southern margin of Eurasia. The blocks termed the Cimmerian Continent separated from Gondwanaland in the late Permian (250 MYBP), migrated northward across the Tethys Sea, and subsequently broke apart along the way. The individual blocks collided with Eurasia, most of which completed suturing from the late Triassic to the middle Jurassic (225–175 MYBP; for details see Sengör, 1984; Sengör *et al.*, 1988). These blocks now are situated from Turkey through Iran, Afghanistan, and Tibet.

The mountain systems of the Iranian Plateau were formed on pre-Eocene plate boundaries by the Indian and Arabian collisions (Fig. 6). The Indian collision

caused the formation of the trans-Himalaya (Hindu Kush, Karakorum, and Himalaya) and the subsequent Pamir–Tien Shan uplift (10 MYBP, Abdrakhmatov *et al.*, 1996) in the region where the two outgroup taxa occur (*L. himalayana* and *L. lehmanni*) (Fig. 6). The more recent Arabian collision caused the uplifting of the Zagros, Lesser Caucasus, Balkhans, and Kopet-Dagh mountains on the margins of the Iranian Plateau. The Zagros Mountains in the south where *L. microlepis* occurs began uplifting in the late Miocene (10 MYBP) (Sborshchikov *et al.*, 1981). In the beginning of the Pliocene (5 MYBP), the Arabian Plate accelerated separation from Africa (Girdler, 1984) and mountain building on the northern (Lesser Caucasus Mountains, Kopet-Dagh) and southern (Zagros) margins of the Iranian Plateau occurred. This activity was most intense in the middle Pliocene (3–4 MYBP). The Pliocene mountain uplifts caused eastern Iran (Lut Plate) to sink (Fig. 6).

The geologic history considered together with our phylogenetic results suggests that an early north-south split separated *L. microlepis* from both *L. erythrogastra* and *L. caucasia* in the late Miocene or early Pliocene (5–10 MYBP). In the north, mountain uplifting was most intense in the middle Pliocene (3–4 MYBP). In particular, in the eastern Kopet-Dagh a sharp uplift occurred in the middle Pliocene (Sborshchikov *et al.*, 1981) and may have fragmented *L. erythrogastra* from *L. caucasia*. The uplifting in the western Kopet-Dagh was more gradual and these mountains spread out over a wider area, suggesting a later Pliocene (2–3 MYBP) formation (Sborshchikov *et al.*, 1981), which is consistent with the phylogenetic hypothesis (Fig. 5). Note that the Balkhan Mountains are a peripheral portion of the western Kopet-Dagh uplift and may have formed even later, perhaps 1–2 MYBP.

Dating Fragmentation of *Laudakia* Populations

Relationships of *Laudakia* populations on the Iranian Plateau are well resolved. Phylogenetic divergences correspond to geologic events that can be dated accurately to within a million years except the fragmentation of *L. microlepis* from the northern populations (*L. caucasia* and *L. erythrogastra*), the north-south split caused by the rise of the Zagros Mountains. If a molecular clock can be assumed, nucleotide substitutions may be useful in narrowing this date of 5–10 MYBP. One indication that DNA sequences are diverging in a clock-like fashion is the congruence of distance-based trees that assume a molecular clock (Kitch) and trees that do not assume a molecular clock (Fitch) (see the documentation in PHYLIP, Felstenstein, 1995). Kitch and Fitch trees generated using nucleotide substitutions were identical in topology to the most parsimonious tree and both methods gave similar branch lengths (results not shown). This observation suggests

that the sequences sampled are evolving in a clock-like manner.

A plot of nucleotide substitutions against times of expected divergence between populations based on geologic history for four nodes are presented in Fig. 7. Considering the error involved in both the timing of geologic events and the consistency of a clock-like substitution pattern, a surprisingly tight fit to the curve is observed ($r^2 = 0.997$). This result provides further evidence that our estimations of geologic events are correct. Interpolation from the curve provides a date of ~9 MYBP for the divergence of *L. microlepis* from the northern populations of *Laudakia*. We calculate a rate of evolution of 0.65% change per lineage per million years (a possible range of 0.61–0.70% given uncertainty in geological dating) for this segment of the mitochondrial genome. This result is compatible with the range of rates (0.5–1.0% change per lineage per million years) provisionally accepted by Moritz *et al.* (1987) based upon data from primates.

An Area Cladogram for the Iranian Plateau

The phylogenetic tree for *Laudakia* is consistent with geologic history and suggests a general biogeographic hypothesis for the faunas of the Iranian Plateau and Pamir, which should constitute sister taxa. Area relationships of the Iranian Plateau (Fig. 8) inferred from *Laudakia* suggest that populations from the Zagros Mountains are the sister taxon to all northern popula-

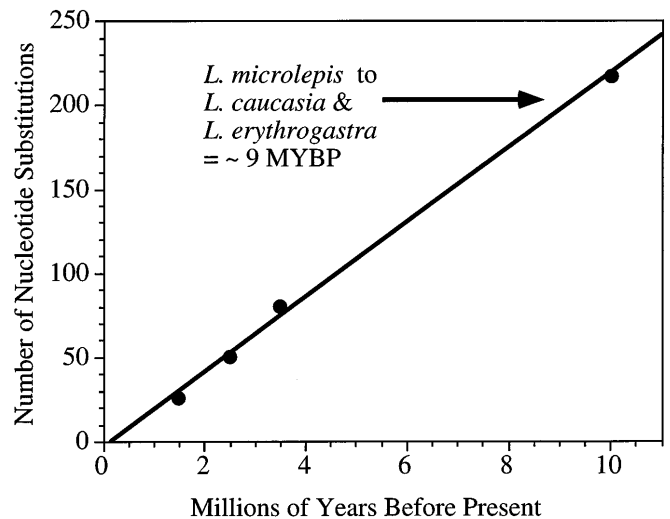


FIG. 7. Plot of nucleotide substitutions against time derived from geologic history. Nucleotide substitutions are an average of all pairwise comparisons across a particular branch. Dates are averaged: 1.5, 1–2 MYBP; 2.5, 2–3 MYBP; and 3.5, 3–4 MYBP. The regression equation is $y = 22.3x - 3.6$. The rate of evolution for this segment of mtDNA is 0.65% change per lineage per million years. When the lower time estimates of averaged dates are used a rate of 0.61% change per lineage per million years is obtained, and when the upper time estimates of averaged dates are used a rate of 0.70% change per lineage per million years is obtained.

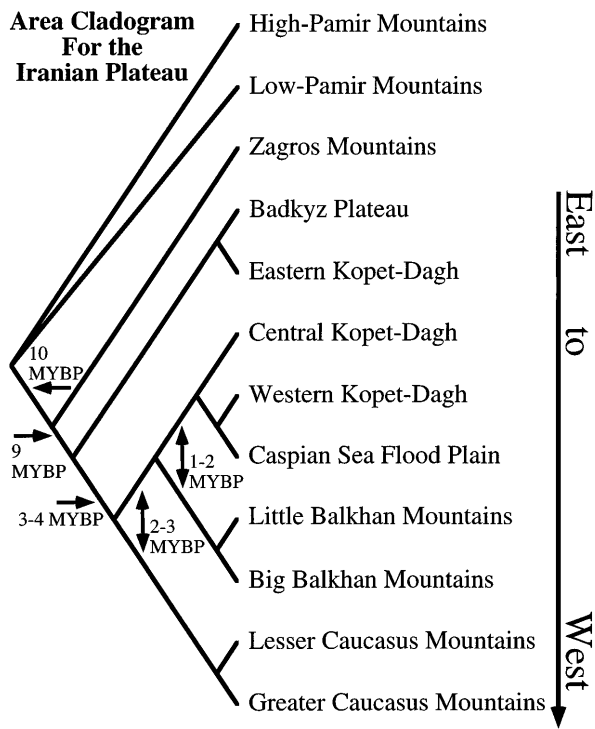


FIG. 8. Area cladogram for the Iranian Plateau. Approximate dates for branching events are shown. The Pamir is shown to root the tree. The fauna of the Zagros is hypothesized to have separated from that in the north during the late Miocene (9 MYBP). In the middle Pliocene (3–4 MYBP) the fauna of the eastern Kopet-Dagh may have separated from other northern areas. Shortly after this event the fauna in the Lesser Caucasus Mountains may have separated from the Kopet-Dagh fauna in the late Pliocene (2–3 MYBP). With continued uplifting in the northern portion of the Iranian Plateau (1–2 MYBP), the fauna of the Balkhan mountains may have diverged from the western Kopet-Dagh. The Greater Caucasus Mountains were an island until the late Pliocene and populations of *Laudakia* were colonized from the Lesser Caucasus Mountains. The Caspian Sea floodplain was submerged until the late Pliocene and was colonized from the western Kopet-Dagh.

tions. This branching event probably occurred 9 MYBP. Populations from the eastern Kopet-Dagh Mountains and the Badkyz Plateau form the sister group to populations from all areas to the west. This branching event is suggested to have occurred 3–4 MYBP. Populations from the Lesser Caucasus Mountains form the sister taxon to those from the mountains of western Turkmenistan. The populations in the western Kopet-Dagh became separated in the late Pliocene (2–3 MYBP), and the Balkhan mountains populations represent a recent split of perhaps 1–2 MYBP.

The Iranian Plateau may be an ideal place for investigating phylogenetic and biogeographic processes because its geologic history suggests successive splitting events well spaced in geologic time. Wide temporal spacing of splitting events provides an ideal situation for phylogenetic reconstruction. If fragmentation of populations occurs too rapidly in temporal succession,

relatively short branches will result and will be difficult to distinguish from a true radiation of populations in which no hierarchy of branching exists.

We propose that the area cladogram for *Laudakia*, featuring a basal north–south split, may be a general one for the fauna of the Iranian Plateau. Future phylogenetic studies of additional fauna from the Iranian Plateau can test this hypothesis. The herpetofauna of the Iranian Plateau is very rich and shows a high degree of endemism (Anderson, 1974; Latifi, 1984), providing an opportunity to test this hypothesis with many taxa.

APPENDIX

Trees used as alternative hypotheses in Templeton (1983) tests. Taxon names appear as in Figure 5. Lengths of trees and consistency indices (CI) (Swofford, 1993) are given in parentheses.

The most parsimonious tree derived by constraining taxa to successive branching patterns around the Iranian Plateau when rooted in the northeast (622 steps, CI 0.764): (*L. himalayana*, (*L. lehmanni*, (((*L. microllepis*, (*L. caucasia*-Dagestan, *L. caucasia*-Armenia)), (*L. caucasia*-central Kopet-Dagh, *L. caucasia*-western Kopet-Dagh, *L. caucasia*-Caspian Sea floodplain)), (*L. caucasia*-Little Balkhan, *L. caucasia*-Big Balkhan))), (*L. erythrogastra*-Badkyz, *L. erythrogastra*-eastern Kopet-Dagh)))).

The most parsimonious tree derived by constraining taxa to successive branching patterns around the Iranian Plateau when rooted in the southeast (564 steps, CI 0.842): (*L. himalayana*, (*L. lehmanni*, (*L. microllepis*, (((*L. erythrogastra*-Badkyz, *L. erythrogastra*-eastern Kopet-Dagh), ((*L. caucasia*-central Kopet-Dagh, (*L. caucasia*-western Kopet-Dagh, *L. caucasia*-Caspian Sea floodplain)), (*L. caucasia*-Little Balkhan, *L. caucasia*-Big Balkhan))), (*L. caucasia*-Dagestan, *L. caucasia*-Armenia)))).

ACKNOWLEDGMENTS

This work was supported by grants from the National Science Foundation (predoctoral fellowship to J.R.M.; DEB-9318642 to J. B. Losos, K. de Queiroz, and A.L.), National Geographic Society (4110-89 and 4872-93 to T.J.P. and J.R.M.), Russian Foundation for Basic Research (N97-04-50093 to N.B.A.), and the California Academy of Sciences. Steven C. Anderson kindly provided unpublished distributional data for Iranian localities. Todd Jackman assisted with analysis of DNA substitutions. We thank Nikolai Orlov and Boris S. Tuniyev for field assistance.

REFERENCES

- Abdrakhmatov, K. Ye., Aldazhanov, S. A., Hager, B. H., Hamburger, M. W., Herring, T. A., Kalabaev, K. B., Makarov, V. I., Molnar, P., Panasyuk, S. V., Prilepin, M. T., Reilinger, R. E., Sadybakasov, I. S., Souter, B. J., Trapeznikov, Yu. A., Tsurkov, V. Ye., and Zubovich, A. V. (1996). Relatively recent construction of the Tien Shan

- inferred from GPS measurements of present-day crustal deformation rates. *Nature* **384**: 450–453.
- Anan'eva, N. B., and Tuniev, B. S. (1994). Some aspects of historical biogeography of Asian rock agamids. *Russ. J. Herpetol.* **1**: 42–52.
- Ananjeva, N. B., and Atayev, Ch. (1984). *Stellio caucasius triannulata* ssp. nov.—A new subspecies of the Caucasian Agama from southwestern Turkmenia. *Tr. Zool. Inst. Akad. Nauk. SSSR* **124**: 4–11. [In Russian]
- Anderson, S. C. (1974). Preliminary key to the turtles, lizards and amphisbaenians of Iran. *Fieldiana: Zool.* **65**: 27–44.
- Anderson, S., Bankier, A. T., Barrell, B. G., de Bruijn, M. H. L., Coulson, A. R., Drouin, J., Eperon, I. C., Nierlich, D. P., Roe, B. A., Sanger, F., Schreier, P. H., Smith, A. J. H., Staden, R., and Young, I. G. (1981). Sequence and organization of the human mitochondrial genome. *Nature* **290**: 457–465.
- Bremer, K. (1994). Branch support and tree stability. *Cladistics* **10**: 295–304.
- Brennicke, A., and Clayton, D. A. (1981). Nucleotide assignment of alkali-sensitive sites in mouse mitochondrial DNA. *J. Biol. Chem.* **256**: 10613–10617.
- Dercourt, J., Zonenshain, L. P., Ricou, L.-E., Kazmin, V. G., Le Pichon, X., Knipper, A. L., Grandjacquet, C., Sborshchikov, I. M., Geyssant, J., Lepvrier, C., Pechersky, D. H., Boulin, J., Sibuet, J.-C., Savostin, L. A., Sorokhtin, O., Westphal, M., Bazhenov, M. L., Lauer, J. P., and Biju-Duval, B. (1986). Geological evolution of the tethys belt from the Atlantic to the Pamirs since the Lias. *Tectonophysics* **123**: 241–315 and maps (plates I–X).
- Felsenstein, J. (1985). Confidence limits on phylogenies with a molecular clock. *Syst. Zool.* **34**: 152–161.
- Felsenstein, J. (1995). "PHYLP: Phylogeny inference package. Version 3.572," University of Washington, Seattle.
- Girdler, R. W. (1984). The evolution of the Gulf of Aden and Red Sea in space and time. *Deep-Sea Res. Part A* **31**: 747–762.
- Hixson, J. E., Wong, T. W., and Clayton, D. A. (1986). Both the conserved and divergent 5'-flanking sequences are required for initiation at the human mitochondrial origin of light strand replication. *J. Biol. Chem.* **261**: 2384–2390.
- Kumazawa, Y., and Nishida, M. (1993). Sequence evolution of mitochondrial tRNA genes and deep-branch animal phylogenetics. *J. Mol. Evol.* **37**: 380–398.
- Larson, A. (1994). The comparison of morphological and molecular data in phylogenetic systematics. In "Molecular Ecology and Evolution: Approaches and Applications" (B. Schierwater, B. Streit, G. P. Wagner, and R. DeSalle, Eds.), pp. 371–390, Birkhäuser, Basel, Switzerland.
- Latifi, M. (1984). "The Snakes of Iran." Iran Department of the Environment, Tehran. [In Farsi] (English translation 1991 by Soc. Study Amphib. Reptiles, Oxford, Ohio.)
- Macey, J. R., Larson, A., Ananjeva, N. B., Fang, Z., and Papenfuss, T. J. (1997a). Two novel gene orders and the role of light-strand replication in rearrangement of the vertebrate mitochondrial genome. *Mol. Biol. Evol.* **14**: 91–104.
- Macey, J. R., Larson, A., Ananjeva, N. B., and Papenfuss, T. J. (1997b). Replication slippage may cause parallel evolution in the secondary structures of mitochondrial transfer RNAs. *Mol. Biol. Evol.* **14**: 30–39.
- Macey, J. R., Larson, A., Ananjeva, N. B., and Papenfuss, T. J. (1997c). Evolutionary shifts in three major structural features of the mitochondrial genome among iguanian lizards. *J. Mol. Evol.* **44**: 660–674.
- Macey, J. R., Schulte II, J. A., Larson, A., Fang, Z., Wang, Y., Tuniyev, B. S., and Papenfuss, T. J. (1998). Phylogenetic relationships of toads in the *Bufo bufo* species group from the eastern escarpment of the Tibetan Plateau: A case of vicariance and dispersal. *Mol. Phylogenet. Evol.* **9**: 80–87.
- Macey, J. R., and Verma, A. (1997). Homology in phylogenetic analysis: Alignment of transfer RNA genes and the phylogenetic position of snakes. *Mol. Phylogenet. Evol.* **7**: 272–279.
- Maddison, W. P., and Maddison, D. R. (1992). "MacClade: Analysis of Phylogeny and Character Evolution, Version 3.0," Sinauer, Sunderland, MA.
- Maniatis, T., Fritsch, E. F., and Sambrook, J. (1982). "Molecular Cloning: A Laboratory Manual," Cold Spring Harbor Laboratory Press, Cold Spring Harbor, NY.
- Moritz, C., Dowling, T. E., and Brown, W. M. (1987). Evolution of animal mitochondrial DNA: Relevance for population biology and systematics. *Annu. Rev. Ecol. Syst.* **18**: 269–292.
- Sborshchikov, I. M., Savostin, L. A., and Zonenshan, L. P. (1981). Present plate tectonics between Turkey and Tibet. *Tectonophysics* **79**: 45–73.
- Sengör, A. M. C. (1984). "The Cimmeride Orogenic System and the Tectonics of Eurasia," Special Paper No. 195, Geol. Soc. Am., Boulder, CO.
- Sengör, A. M. C., Altiner, D., Cin, A., Ustaomer, T., and Hsu, K. J. (1988). Origin and assembly of the Tethyside orogenic collage at the expense of Gondwana Land. In "Gondwana and the Tethys" (M. G. Audley-Charles and A. Hallam, Eds.), pp. 119–181, Geol. Soc. Special Pub. No. 37, Oxford Univ. Press, Oxford.
- Swofford, D. L. (1993). "PAUP: Phylogenetic Analysis Using Parsimony, Version 3.1.1," Illinois Natural Hist. Survey, Urbana, IL.
- Tapponier, P., Mattauer, M., Proust, F., and Cassaigneau, C. (1981). Mesozoic ophiolites, sutures, and large-scale tectonic movements in Afghanistan. *Earth Planet. Sci. Lett.* **52**: 355–371.
- Templeton, A. R. (1983). Phylogenetic inference from restriction endonuclease cleavage site maps with particular reference to the evolution of humans and the apes. *Evolution* **37**: 221–244.
- Tuniev, B. S., Atayev, Ch., and Shammakov, S. (1991). *Stellio erythrogaster nurgeldievi* ssp. nov. (Agamidae, Sauria)—A new subspecies from the eastern Kopet-Dagh. *Izv. Akad. Nauk. Turkm. SSR* **6**: 50–60. [In Russian]
- Zar, J. H. (1984). "Biostatistical Analysis," 2nd ed. Prentice Hall International, Englewood Cliffs, NJ.
- Zhang, D.-X., and Hewitt, G. M. (1996). Nuclear integrations: Challenges for mitochondrial DNA markers. *Trends Ecol. Evol.* **11**: 247–251.